International Journal of Coal Geology 100 (2012) 51–64

Contents lists available at SciVerse ScienceDirect

International Journal of Coal Geology

journal homepage: www.elsevier.com/locate/ijcoalgeo

Pore size distribution and accessible pore size distribution in bituminous coals

Richard Sakurovs [a,*], Lilin He [b], Yuri B. Melnichenko [b], Andrzej P. Radlinski [c,d], Tomas Blach [d], Hartmut Lemmel [e], David F.R. Mildner [f]

[a] CSIRO Energy Technology, 11 Julius Avenue North Ryde 2113 NSW, Australia
[b] Biology and Soft Matter Division, Neutron Scattering Directorate, Oak Ridge National Laboratory, Oak Ridge, TN 37831-6393, USA
[c] Indiana Geological Survey, Indiana University, Bloomington, Indiana 47405-2208, USA
[d] Queensland Micro and Nanotechnology Centre, Griffith University, Nathan 4111, Brisbane, Australia
[e] Institut Laue-Langevin 38000 Grenoble, France
[f] Center for Neutron Research, National Institute of Standards and Technology, Gaithersburg, MD 20899, USA

ARTICLE INFO

Article history:
Received 28 March 2012
Received in revised form 18 June 2012
Accepted 18 June 2012
Available online 27 June 2012

Keywords:
SANS
Coal porosity
Maceral composition
Methane accessibility
Coal microstructure
Closed porosity

ABSTRACT

The porosity and pore size distribution of coals determine many of their properties, from gas release to their behavior on carbonization, and yet most methods of determining pore size distribution can only examine a restricted size range. Even then, only accessible pores can be investigated with these methods. Small-angle neutron scattering (SANS) and ultra small-angle neutron scattering (USANS) are increasingly used to characterize the size distribution of all of the pores non-destructively. Here we have used USANS/SANS to examine 24 well-characterized bituminous and subbituminous coals: three from the eastern US, two from Poland, one from New Zealand and the rest from the Sydney and Bowen Basins in Eastern Australia, and determined the relationships of the scattering intensity corresponding to different pore sizes with other coal properties. The range of pore radii examinable with these techniques is 2.5 nm to 7 μm. We confirm that there is a wide range of pore sizes in coal. The pore size distribution was found to be strongly affected by both rank and type (expressed as either hydrogen or vitrinite content) in the size range 250 nm to 7 μm and 5 to 10 nm, but weakly in intermediate regions. The results suggest that different mechanisms control coal porosity on different scales. Contrast-matching USANS and SANS were also used to determine the size distribution of the fraction of the pores in these coals that are inaccessible to deuterated methane, CD_4, at ambient temperature. In some coals most of the small (~10 nm) pores were found to be inaccessible to CD_4 on the time scale of the measurement (~30 min–16 h). This inaccessibility suggests that in these coals a considerable fraction of inherent methane may be trapped for extended periods of time, thus reducing the effectiveness of methane release from (or sorption by) these coals. Although the number of small pores was less in higher rank coals, the fraction of total pores that was inaccessible was not rank dependent. In the Australian coals, at the 10 nm to 50 nm size scales the pores in inertinites appeared to be completely accessible to CD_4, whereas the pores in the vitrinite were about 75% inaccessible. Unlike the results for total porosity that showed no regional effects on relationships between porosity and coal properties, clear regional differences in the relationships between fraction of closed porosity and coal properties were found. The 10 to 50 nm-sized pores of inertinites of the US and Polish coals examined appeared less accessible to methane than those of the inertinites of Australian coals. This difference in pore accessibility in inertinites may explain why empirical relationships between fluidity and coking properties developed using Carboniferous coals do not apply to Australian coals.

© 2012 Published by Elsevier B.V.

1. Introduction

The porosity of coals and the nature of the connections between pores are factors crucial in determining the efficiency of methane extraction from coal beds and the rate of release of fugitive methane emissions from coal mines. Most of the pore volume in coals is due to micropores, that is pores with a minimum width of less than 2 nm, but mesopores (2–50 nm) and macropores (>50 nm) also contribute significantly to the total volume in many cases (Clarkson and Bustin, 1996; Gan et al., 1972). The concept that most of the micro- and mesopores of coal are connected by tightly restricted bottlenecks appears to be generally held (Radovic et al., 1997; White et al., 2005), though an alternative view, that molecules diffuse through coal to otherwise closed pores, has been proposed (Larsen et al., 1995). An intermediate view is that of Chalmers and Bustin (2007) who suggest that because in their study they found that liptinite-rich materials had low accessible micropore volume but high sorption capacity for methane, that gas dissolves in liptinites but not other macerals.

* Corresponding author.
E-mail address: Richard.sakurovs@csiro.au (R. Sakurovs).

0166-5162/$ – see front matter © 2012 Published by Elsevier B.V.
doi:10.1016/j.coal.2012.06.005

However, one unresolved issue is the extent to which the pores are accessible to gases such as methane. Are there pores that are closed to methane, and if so, to what extent? Thimons and Kissell (1973), on the basis of diffusion measurements, have suggested that there are pores that are accessible to helium but not to methane. Some have drawn an even finer distinction by suggesting that there are pores in coal that carbon dioxide can penetrate that methane cannot (Cui et al., 2004; Narkiewicz and Mathews, 2009), either because the carbon dioxide molecules are narrower than methane or because CO_2 plasticizes the coal (Larsen, 2004). The former explanation is not true for the coals investigated by Sakurovs et al. (2010) who found that, though their methane sorption capacity was much less than that for CO_2, the capacity for the coals to sorb xenon and ethane was similar to that of CO_2, even though they are larger molecules than even CH_4. Only when still larger molecules – CF_4 and SF_6 – were used, did reduction of sorption capacity by decreasing pore access become important.

The issue of inaccessible or 'blind' pores is important because it determines the overall extraction efficiency of methane from coal. When the coal is formed, methane can be produced and trapped in these pores, but if the pores are closed the gas cannot escape from the coal. However, in some standard methods 'total' gas release determination is done by crushing the coal finely (Diamond and Schatzel, 1998), which will open some fine pores and allow the gas trapped within them to escape. Powdering the coal may therefore result in overestimating the amount of gas that can be extracted from coal seams.

Small-angle neutron scattering (SANS) and ultra small-angle neutron scattering (USANS) are increasingly used to characterize, non-destructively, the pore size distribution of materials over the size range 1 nm to 10 μm. SANS and USANS record the scattering from *all* pores, including pores that are inaccessible to fluids and therefore cannot be measured with techniques that involve gas sorption or fluid intrusion, such as mercury porosimetry. The scattering is dependent on differences in the neutron scattering length density (SLD) within the sample, with the major contribution being from pores, where the contrast between the solid material and the pore is large. Smaller pores scatter neutrons at larger angles. In SANS, the most abundant minerals and organics in coal have a similar scattering length density (Radlinski, 2006). Thus scattering from mineral inclusions in coal contributes much less to the total scattering intensity than do pores in the coal. Scattering intensity increases as the square of the difference in SLD between the pore and its host material (Radlinski et al., 2000). Since scattering from hydrogen produces an angle-independent background that is comparable or greater in intensity to scattering from fine pores, in most coals the smallest pores accessible by SANS investigations have a radius of about 2.5 nm (Radlinski, 2006). This restricts direct SANS investigations of coal to meso and macropores. Investigation of smaller pores in coals using SANS requires extrapolation (Mares et al., 2009). However, extrapolation from meso and macropores may not give accurate results.

There have been several studies investigating the SANS of coals (Gethner, 1986; Mares et al., 2009; Mirzaeian et al., 2010; Radlinksi et al., 2009), but most have concentrated on detailed characterization of one coal or a limited range of coals. In the most extensive study, Tricker et al. (1983) investigated nine American and British coals of rank ranging from lignite to semi-anthracite and found that the scattering intensity corresponding to a pore size of 500 nm was greatest from coals with nearly 80% carbon. Hall et al. (2000), on the basis of measurements on five Argonne premium coals concluded that the scattering intensity decreases with increasing rank and that microporosity is absent in the high rank Pocahontas #3. However, this seems unlikely in view of its ability to sorb gases (Mohammad et al., 2011). Prinz et al. (2004) studied samples of eight coals ranging from medium volatile bituminous to anthracite from the Ruhr basin and confirmed that the amount of meso and macropores decreases with increasing rank in this rank region. The lower mesoporosity in coals of less than 75% carbon compared to higher rank coals may be a consequence of the drying process (Spitzer, 1981), which irreversibly shrinks low rank coals. Setek et al. (1983) suggests that for low rank coals scattering experiments should be performed on bed-moist coals.

Recent developments have allowed SANS and USANS to be able to discriminate between pores accessible to gases and those inaccessible to gases (Melnichenko et al., 2012). Information on the inaccessible porosity is obtained using the technique of contrast matching. In this case the system consists of two components: the solid coal matrix and the pore-invading fluid. The scattering intensity from such a two-component system is proportional to the square of the difference in the SLD of the two phases. If SLDs of the two components are equal (the zero contrast (ZC) or contrast-matching condition), the scattering of all pores accessible to the contrast matching fluid is annulled, leaving scattering only from inaccessible pores. For CD_4 fluid invading coals, the pressures required to achieve ZC at room temperature are of the order of 3000–6000 psig [(20–40) MPa]. The ratio of number of inaccessible pores to the number of total pores is the ratio of signal intensity at the ZC condition to the signal intensity obtained in a vacuum.

A common problem in determining relationships between the properties of coal is that many of their properties are dependent on a range of factors, such as rank, maceral composition, mineral matter and where and when they were formed, values that are often correlated especially when only a small number of samples from one location are investigated. This makes disentangling general relationships a challenge. In this paper we have measured the USANS and SANS of 24 bituminous coals, covering a wide range of rank, origin and maceral composition, and examined the relationships between them. Using contrast matching techniques, we have also determined the fraction of pores of these coals that are inaccessible to methane as a function of pore size and compared these with other coal properties.

2. Materials and methods

2.1. Samples

Twenty-four coal samples were investigated in this study; two from Poland, three from the US (Appalachian), one from New Zealand and the rest from the Bowen and Sydney basins, Australia. They are commercial samples that have been washed to reduce mineral matter levels. The coal samples were prepared in the form of particulates with the particle size −1 + 0.5 mm which were used for all analytical characterization (Table 1). Other data for these coals is listed elsewhere (Day et al., 2008). The daf carbon contents of the coals ranged between 80 and 90% and the mean maximum vitrinite reflectance (R_v,max) between 0.69% and 1.63%.

2.2. Neutron scattering measurements

Prior to measurements the samples were dried for a few hours under vacuum at 60 °C to remove moisture. Measurements on the unpressurized coals reported here were performed with coal particles in stoppered quartz cells with a 2 mm internal spacing, for all coals except coal 7. Closed porosity measurements were determined in a second series of experiments for all coals except for coal 1. For this series of experiments samples were loaded into thin-wall aluminum holders with internal thickness 1 mm and then placed in a SANS/USANS pressure cell. The SANS and USANS scattering profiles of coals were collected in vacuum and at the pressure calculated to achieve zero average contrast. The pressure was increased using a pressure intensifier, to the required pressure of CD4 (Table 1). Each

Table 1
Analytical data for coals. Also included are the SLD values for each coal and the pressure of CD_4 required to reach the zero average contrast condition for contrast matching.

	Source	Ash	Helium density	Carbon	Hydrogen	Volatile matter	R_v,max	Vitrinite	Liptinite	SLD	P_{ZC} at 23 °C
		db, %	kg m^{-3}	daf, %	daf,%	daf, %	%	mmf, %	mmf, %	10^{10} cm^{-2}	MPa
1	Australia	6.6	1.353	85.87	5.09	29.3	1.06	65.1	2.2	2.64	29
2	Australia	7.7	1.422	82.99	4.66	31.7	0.69	29.7	3.9	2.87	33
3	Australia	12.0	1.350	81.70	5.74	41.4	0.79	84.2	4.1	2.35	24
4	NZ	2.5	1.295	85.95	5.63	35.2	1.11	95.5	2.0	2.34	24
5	Australia	20.3	1.594	80.68	3.93	31.2	0.62	23.9	1.6	3.47	51
6	Australia	8.3	1.391	85.61	4.93	30.0	0.90	33.9	2.3	2.76	31
7	Australia	8.9	1.375	88.80	4.95	24.5	1.27	48.7	0.4	2.77	31
8	Australia	6.4	1.357	88.35	4.83	23.5	1.29	59.1	0.2	2.77	31
9	Australia	9.1	1.368	89.22	5.37	27.7	1.21	85.4	0.3	2.63	29
10	Australia	7.4	1.348	87.90	5.24	27.0	1.16	69.1	1.1	2.61	28
11	Australia	5.6	1.313	84.11	5.73	36.1	0.95	82.7	4.1	2.33	24
12	Australia	6.1	1.293	83.17	5.88	45.8	0.70	68.3	14.1	2.38	25
13	Australia	7.4	1.331	83.59	5.40	37.3	0.89	88.7	2.2	2.46	26
14	Australia	8.4	1.376	88.76	4.87	20.4	1.63	83.9	0.0	2.8	32
15	Australia	10.0	1.365	85.67	5.27	31.9	1.08	74.3	2.3	2.6	28
16	Australia	8.8	1.367	88.82	5.01	23.4	1.43	76.7	0.0	2.74	31
17	Australia	5.1	1.334	86.30	5.50	31.2	1.03	63.6	1.7	2.48	26
18	Australia	7.2	1.316	86.64	5.50	32.7	0.99	90.9	0.7	2.45	26
19	Australia	21.3	1.473	83.23	5.03	37.5	0.77	61.8	4.8	2.84	33
20	USA	5.1	1.357	89.67	4.75	19.7	1.61	81.7	0.1	2.8	32
21	USA	4.1	1.312	85.92	5.56	36.4	0.98	72.5	7.0	2.4	26
22	USA	5.3	1.324	84.37	5.55	38.5	0.90	89.4	3.5	2.4	26
23	Poland	5.7	1.365	89.61	4.73	22.8	1.34	35.6	3.3	2.83	33
24	Poland	5.8	1.363	88.96	4.73	24.8	1.22	47.6	4.2	2.81	32

measurement began 10 min after increasing the pressure to allow equilibrium saturation of pores with the injected fluid. This equilibration time was determined in separate kinetics experiments in which the intensities of scattering for coals 5 and 11 were measured as a function of time during 16 h after changing the pressure. No changes in scattering patterns were observed at times longer than 10 min after the fluid injection. After the determinations at pressure, some samples were re-evacuated and remeasured. No difference was observed between the results in vacuum before and after pressure was applied, indicating the pressure effects were reversible and that there was little loosely bound water remaining in the sample after the initial drying step, since if water were present, some would have been removed during the depressurization step and the SANS profiles would have changed.

All SANS experiments were conducted using the General-Purpose SANS instrument at Oak Ridge National Laboratory (http://neutrons.ornl.gov/instruments/HFIR/CG2/), with neutron wavelengths λ of 1.2 nm and 0.48 nm (Δλ/λ~0.13). Fig. 1 summarizes the measurement procedure. Sample to detector distances were chosen to cover an overall range of scattering vectors (Q) $0.0016<Q<0.2\,Å^{-1}$, where $Q=(4\pi/\lambda)sin(\theta/2)$ and θ is the scattering angle. The acquisition time from the coals varied from approximately 10 min to an hour at each detector position to ensure sufficient data statistics. The raw 2D data were corrected for the detector pixel efficiency and dark current, which represents the ambient radiation background and electronic noise, and azimuthally averaged to produce a 1D profile, I(Q). Data were placed on an absolute scale in units of cm^{-1} through the use of pre-calibrated standard polymethyl methacrylate and porous silica. All the USANS measurements on the first series of unpressurized coals were carried out were carried out at the Institut Laue-Langevin (ILL), Grenoble, France, using a neutron wavelength of λ = 1.92 Å (Q range $2.5\times10^{-5}<Q<0.003\,Å^{-1}$) (http://www.ill.eu/instruments-support/instruments-groups/instruments/s18/characteristics/). For the second series of experiments, which involved comparisons of results on coal exposed to CD_4 with the same coals under vacuum, measurements under vacuum and at pressure were measured on the same sample in the same cell sequentially. USANS measurements on six samples (samples 1, 13, 17, 20, 21 and 22) were carried out at National Institute of Standards, Gaithersburg, Maryland, USA, using the BT5 perfect crystal SANS instrument with a wavelength λ = 2.38 Å (with a Q range $3\times10^{-5}<Q<0.003\,Å^{-1}$) (http://www.nist.gov/ncnr/bt5-usans-ultra-small-angle-neutron-scattering.cfm) and the other samples at ILL After desmearing, the normalized data were merged with the SANS data. Application of the instruments in tandem allows the neutrons to probe a broad range of pore sizes. Q was converted to pore radius (R) using the approximate relationship,

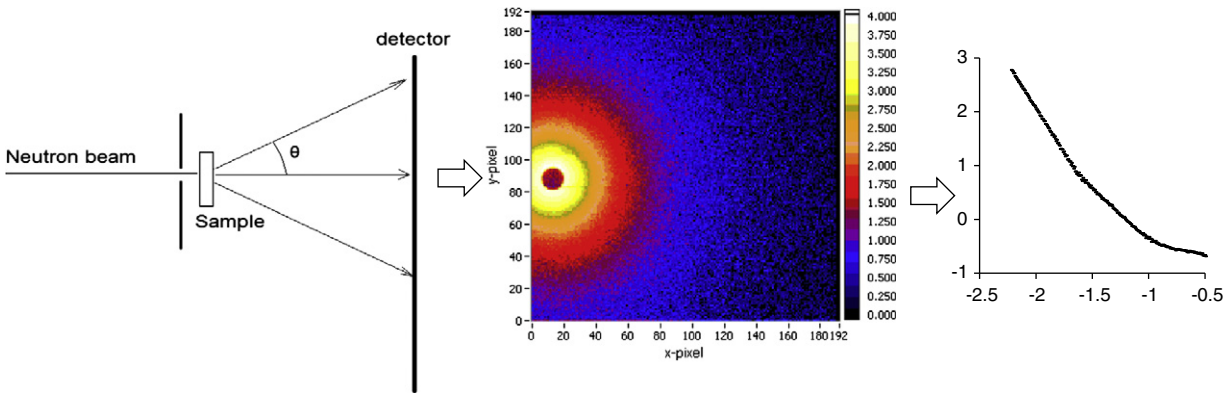

Fig. 1. Summary of the small angle neutron scattering measurement.

R=2.5/Q (Radlinski et al., 2000). Thus the accessible R values range from 0.8 nm to 10 μm.

The SLD of each coal (Table 1) was calculated based on their chemical composition and matrix (helium) density d:

$$\mathrm{SLD} = N_A d \sum_i s_i b_i / \sum_i s_i M_i \quad (1)$$

where N_A is Avogadro's constant, s_i is the proportion by number of nucleus i in the coal, M_i is its atomic mass, and b_i is the coherent scattering amplitude for nucleus i. Zero contrast pressure (P_{ZC}) is defined as the pressure at which the SLDs of the solid matrix of coal and the fluid are equal. The SLD of CD_4 is $[10\cdot(\rho_{CD4})]\ 10^{10}\,\mathrm{cm}^{-2}$ where ρ_{CD4} is the density of CD_4 (g/cm^3). The pressures that provide density corresponding to the zero average contrast condition were calculated using equations of state of CH_4 using the REFPROP software obtained from NIST (http://www.nist.gov/data/nist23.htm). Assuming that the molar density for both CH_4 and CD_4 are the same at each pressure, the densities of deuterated methane CD_4 are calculated from densities of normal methane by multiplying by a factor 1.25 (the ratio of atomic weights of CD_4 and CH_4). Because the scattering intensity from the pore/matrix interface is proportional to the square of the scattering length density difference, the scattering intensity is not sensitive to small differences in pressure near the zero contrast condition – a 5% departure in pressure from P_{ZC} would lead to less than 1% difference in scattering intensity relative to the intensity in vacuum. Therefore, for the purpose of determining the proportion and size distribution of inaccessible pores exact contrast matching is not essential. Helium density is used to determine the molar mass, and it has been suggested that helium does not penetrate all of the micropores in coals. A previous study on coals has shown good agreement between calculated and measured zero contrast pressure on coals (Melnichenko et al., 2012) suggesting that errors in the calculation of SLD introduced by microporosity inaccessible to helium are negligible.

3. Results

3.1. Unpressurized coals

Fig. 2 shows the combined USANS/SANS results for four of the coals investigated, selected to show the greatest differences in results. Other samples showed results that were generally intermediate between the results for these coals. In these coals, I(Q) varies by over ten orders of magnitude, and is approximately linear on a log–log scale over the range of R of 10 to 10,000 nm.

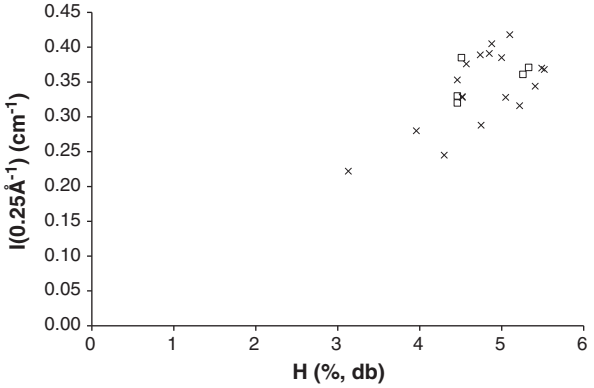

Fig. 3. Relationship between scattering intensity at R=1 nm (or Q=0.25 Å^{-1}) and hydrogen content of coals (x=Southern hemisphere coals, □=Northern hemisphere coals).

At large pore sizes, there is a tendency for the scattering to level off in some coals. This could be due either to a relative paucity of large pores (>5 μm) or to multiple scattering effects. For this reason measurements at R>8000 nm were not used in further analysis. Below 5 nm, I(Q) becomes independent of R. This is due to a contribution from incoherent scattering (which introduces an angle-independent background) and possibly small scale (<1 nm) inhomogenieties such as micropores. The value chosen for the background scattering was I(Q) at R value of 1 nm. Except for coals 2 and 6, I(Q) changed little between 1 and 4 nm. If incoherent scattering was the only source of scattering at these pore sizes, then the incoherent scattering should increase with the hydrogen content of the coal. Fig. 3 shows I(Q) at an R value of 1 nm does increase with increasing hydrogen content, but other factors such as heterogeneities on size scales <1 nm appear almost as important in determining the intensity of this scattering (see below). Because at small pore sizes most of the scattering contribution was due to background, analysis of the I(Q) values corrected for background was restricted to R>2.5 nm.

Fig. 4 shows the I(Q) values after the background scattering has been subtracted. Coals 2 and 5 show a distinct flattening of the slope below R values of 10 nm, suggesting that pore of this size are more common than expected from linear extrapolation of the results for large pores. These coals are also of lowest rank. Similar results for other low rank coals have been observed previously (Radlinski et al., 2004). Coals 2 and 5 also exhibit a greater scattering intensity than the other coals over the entire size range. This is partly due to the greater SLD of these coals – if pores are empty the scattering intensity

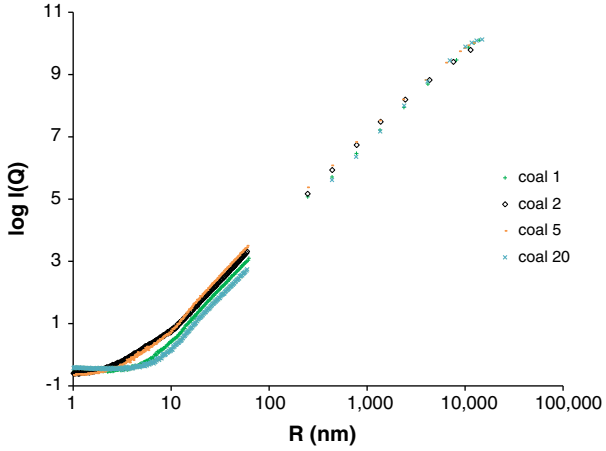

Fig. 2. Combined SANS/USANS data for 4 coals. R is set to 2.5/Q to provide a graphical depiction of pore radius.

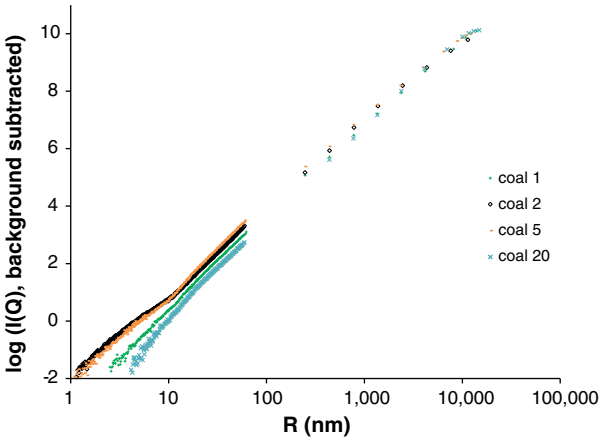

Fig. 4. Plot of I(Q) versus pore radius (R=2.5/Q) for the four coals after subtraction of background.

Table 2
Slopes of neutron scattering data at various Q ranges and I(Q) intensities at various Q values for the coals investigated.

	α	α	α	α	α	$I(10^{-4}Å^{-1})/SLD^2$	$I(10^{-3}Å^{-1})/SLD^2$	$I(0.01Å^{-1})/SLD^2$	$I(0.062Å^{-1})$	$I(0.1Å^{-1})$	$I(0.15Å^{-1})$	$I(0.25Å^{-1})$
R range	2.5–8000	250–8000	20–80	12–20	5–12	*	*	*				
Units	nm	nm	nm	nm	nm	$10^{-14}cm^3$	$10^{-17}cm^3$	$10^{-20}cm^3$	cm^{-1}	cm^{-1}	cm^{-1}	cm^{-1}
Associated pore radius (nm)						2500	250	25	4	2.5	1.7	1
1	−3.35	−3.05	−3.28	−3.67	−3.35	15.56	13.67	8.97	0.42	0.31	0.40	0.29
2	−2.94	−3.06	−3.33	−3.33	−2.22	22.49	19.73	13.52	0.97	0.45	0.30	0.25
3	−3.18	−3.24	−3.01	−3.52	−3.18	18.05	11.90	11.13	0.49	0.37	0.34	0.33
4	−3.38	−3.43	−3.23	−3.38	−3.62	18.08	6.70	4.12	0.41	0.38	0.37	0.37
5	−3.12	−2.92	−3.39	−3.81	−2.51	19.12	23.25	15.40	0.78	0.34	0.26	0.22
6	−3.29	−3.11	−3.45	−3.92	−2.92	14.04	10.78	8.19	0.47	0.35	0.35	0.33
8	−3.44	−3.36	−3.10	−4.00	−3.40	16.97	16.32	9.45	0.38	0.32	0.32	0.33
9	−3.48	−3.29	−3.46	−3.57	−3.57	16.65	8.58	3.53	0.43	0.38	0.39	0.41
10	−3.44	−3.17	−3.38	−4.03	−3.45	23.11	15.73	7.79	0.40	0.36	0.36	0.39
11	−3.20	−3.26	−3.09	−3.51	−3.24	15.42	8.47	5.68	0.43	0.39	0.38	0.34
12	−3.29	−3.29	−3.14	−3.68	−3.37	26.35	13.80	8.97	0.49	0.41	0.41	0.37
13	−3.30	−3.31	−3.16	−3.56	−3.21	14.63	7.20	5.81	0.44	0.39	0.37	0.39
14	−3.47	−3.36	−3.35	−3.63	−3.50	13.34	5.92	3.12	0.36	0.33	0.33	0.35
15	−3.41	−3.34	−3.23	−3.81	−3.38	20.59	9.28	5.35	0.44	0.39	0.38	0.39
16	−3.50	−3.28	−3.40	−3.99	−3.51	19.72	10.50	4.85	0.38	0.33	0.35	0.38
17	−3.19	−3.10	−3.24	−3.52	−2.88	30.39	23.97	10.44	0.52	0.37	0.34	0.32
18	−3.36	−3.28	−3.33	−3.49	−3.10	18.98	10.01	3.76	0.48	0.42	0.44	0.42
19	−3.26	−3.13	−3.19	−3.61	−3.09	35.36	25.97	15.01	0.51	0.34	0.29	0.28
20	−3.45	−3.33	−3.20	−3.97	−3.94	14.70	8.94	4.36	0.37	0.36	0.36	0.39
21	−3.33	−3.11	−3.02	−4.01	−3.39	14.75	11.45	11.77	0.48	0.39	0.38	0.37
22	−3.23	−3.30	−3.16	−3.78	−3.17	15.91	7.90	5.84	0.48	0.40	0.38	0.36
23	−3.51	−3.32	−3.19	−3.94	−3.55	14.77	7.04	5.59	0.36	0.30	0.30	0.32
24	−3.42	−3.29	−3.26	−3.74	−3.40	19.31	9.90	5.61	0.39	0.32	0.32	0.33

I(Q) values normalized for inert mineral matter (see text) *=corrected for background.

is proportional to the square of the SLD of the coal – and partly due to their greater number of pores (see below).

3.1.1. Average slope of the log–log plot

One indicator of the structure of the coal is the slope of the log–log relationship between I(Q) and Q. The fractal surface dimension (Ds) is equal to 6 plus the slope of the log–log plot of I(Q) versus Q. By convention α is negative. For smooth surfaces α is −4, for surface fractals (typified by rough surfaces) α ranges between −3 and −4 and for mass fractals (typified by cracks in solids) α ranges between −2 and −3 (Radlinski, 2006). If the physical structure of a material follows the mass fractal relationship on all scales, then all of the surface of the material would be accessible to the exterior and thus there would be no inaccessible pores (for detailed discussion and references see Radlinski (2006)).

Values of the overall slope (α) were calculated over the range of R of 2.5 nm to 8000 nm. At the small R end, the fit was truncated to the first I(Q) value after which the background-corrected value became negative (due to noise), if this occurred at R values greater than 2.5 nm. Table 2 shows the slopes obtained. The values range between −2.9 and −3.5, indicating that coals range in fractal behavior from mass to surface fractals.

Fig. 5 shows the relationship between α and mean maximum vitrinite reflectance (R_v,max) and vitrinite content. There is a significant and steady decrease in α as R_v,max increases, indicating that the fraction of fine pores decreases as rank increases. There is no such correlation with vitrinite content. This figure shows that in the pore size range 2.5 nm to 8000 nm, variations in slope are more strongly related to R_v,max than maceral composition. A similar trend in decreasing α with increasing rank was seen by Prinz et al. (2004), though the values for α they obtained were somewhat more negative than those reported here, between the range −3.2 and −3.8. There was no systematic variation in α due to origin: American-European Carboniferous and Australian Permian coals were not distinguishable by this criterion.

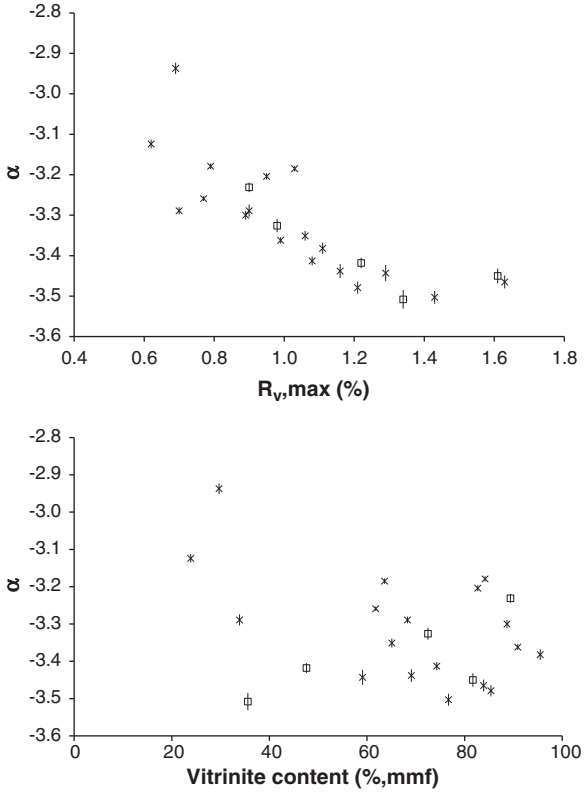

Fig. 5. Relationship between overall slope, α, and mean maximum vitrinite reflectance (R_v,max) and vitrinite content. (x = Southern hemisphere coals, □ = Northern hemisphere coals). Standard errors are indicated.

In view of previous findings that stated quite firmly that maceral composition did play a role in determining the pore size distribution (Clarkson and Bustin, 1996), a more detailed examination of the data was undertaken. For example, it is feasible that if *rank is fixed*, there could be a positive correlation between maceral composition and α. If so, then performing a multiple linear regression using both rank and vitrinite content should significantly increase the r^2 correlation coefficient over that of rank alone. The scattering data was regressed against combinations of coal properties and the multiple r^2 correlation coefficients were determined (Table 3). The increase in r^2 on adding vitrinite as a second independent parameter is not significant. This demonstrates that globally there is no relationship between overall slope of the scattering curve and vitrinite content. This confirms that the shape of the overall pore size distribution in the range 2.5 to 8000 nm in coals is determined largely by rank and not by vitrinite content.

Inspection of Fig. 4 shows that in some cases the slopes of the curves varied with R. In order to investigate this further, the residuals of the linear fit were determined – that is, the difference in log (values) between measured and that obtained by the straight line fit over the full data range (Fig. 6). This allows deviations from linearity in the slopes shown in Fig. 4 to be more readily observed. Fig. 6 shows that using a single value of α is insufficient to completely describe the structure of coals. On this scale, a difference in 0.6 in the residuals corresponds to a factor of 4 in intensity. While there is considerable variation between coals in the relationship between pore size and the residuals of the straight line fit to the log–log relationship, there were a number of common features identified:

1. When R was greater than 250 nm, the residuals tended to be negative, suggesting the slope in this region is less negative than the overall average. In other words, assuming a constant slope over the full size range tends to overestimate the number of >250 nm pores compared to the number of smaller sized pores.
2. For most coals, when R is between 10 and 25 nm the slope is more negative than it is at other R values.
3. When R is less than 8 nm, the slope becomes less negative again. This change is particularly marked for the low carbon coals 2 and 5.

In order to elucidate this behavior the data were partitioned into regions between R values of 250 and 8000 nm, 20 and 80 nm, 12 and 20 nm, and 5 and 12 nm and α determined over these intervals.

3.1.2. Scattering intensity at different pore sizes

The I(Q) intensity was determined at R values of 2500, 250 and 25 nm (from interpolation of the linear fits above). Since at these pore sizes most of the scattering is due to pores, in order to compare

Table 3
Multiple r^2 correlation coefficients between SANS/USANS results and some coal properties.

Parameters	H	V	R	R,V	R,H	C,H	C,H,R,V	C,H,R,V,a
α (overall)	0.0	0.11	0.65	0.66	0.67	0.70	0.74	0.79
α (250, 8000)	0.14	0.39	0.32	0.55	0.56	0.45	0.58	0.58
α (20, 80)	0.22	0.08	0.03	0.15	0.23	0.27	0.38	0.39
α (12, 20)	0.11	0.05	0.16	0.28	0.23	0.26	0.29	0.3
α (5, 12)	0.08	0.33	0.55	0.69	0.72	0.61	0.73	0.74
$I(0.0001\,Å^{-1})/SLD^2$	0	0.03	0.15	0.15	0.15	0.09	0.18	0.42
$I(0.001\,Å^{-1})/SLD^2$	0.10	0.26	0.25	0.4	0.41	0.33	0.42	0.53
$I(0.01\,Å^{-1})/SLD^2$	0.07	0.34	0.46	0.63	0.62	0.57	0.68	0.72
$I(0.062\,Å^{-1})$	0.14	0.3	0.48	0.61	0.72	0.67	0.73	0.75
$I(0.1\,Å^{-1})$	0.14	0.04	0.39	0.54	0.46	0.43	0.56	0.56
$I(0.15\,Å^{-1})$	0.55	0.5	0.03	0.55	0.56	0.57	0.70	0.7
$I(0.25\,Å^{-1})$	0.32	0.58	0.17	0.62	0.59	0.6	0.75	0.76

H = hydrogen (daf), C = carbon (daf), V = vitrinite (mmf), R = R_v,max (%), a = ash yield (db). Correlation coefficients of less than 0.17 are not statistically significant.

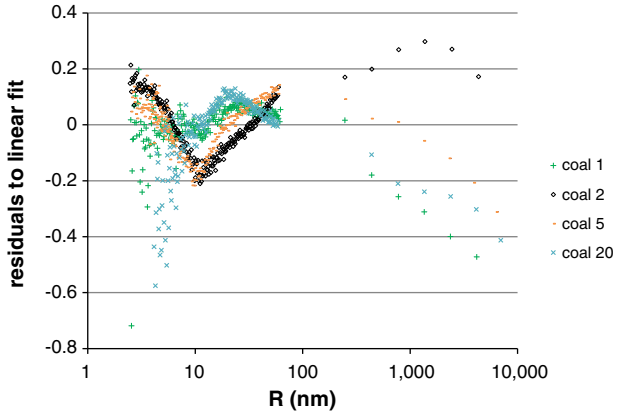

Fig. 6. Residuals to linear fit to the USANS/SANS data.

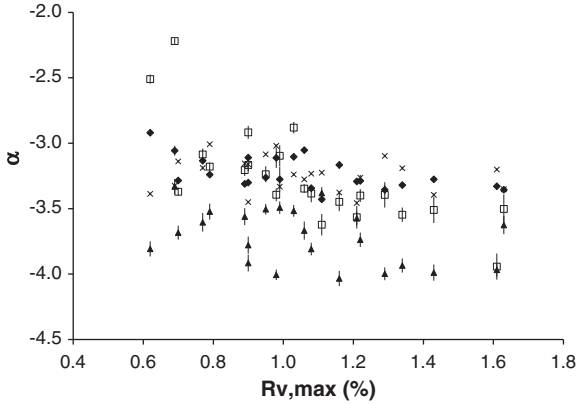

Fig. 7. Slopes of log(I(Q)) versus log(Q) in various size regions, plotted against mean maximum vitrinite reflectance. Diamonds, α(250, 8000); crosses, α(20, 80); triangles, α(12, 20); squares, α(5, 12), where values are expressed as nm. Standard errors are indicated.

scattering intensities with coal properties, which are reported on a mineral matter free basis, the scattering intensity needed to be corrected by two factors.

1. For a given number of pores of a certain size, the intensity of scattering from the pores is proportional to the square of the SLD of the coal. The I(Q) values obtained after background subtraction were divided by the square of SLD.
2. The intensity should also be corrected for the volume of mineral matter (assuming it does not contribute to the scattering). The mineral matter volume fraction can be calculated from the ash yield (a), expressed as a fraction of the total mass, by the relationship

$$\text{Mineral matter volume fraction} = (a/z)/(1-a+a/z) \quad (2)$$

where z is the ratio of mineral matter density to coal density. The correction to the intensity is 1/(1 − mineral matter volume fraction). For typical mineral matter in coals, the density is about 2.6 to 3 and that for coals in the absence of mineral matter, about 1.3 to 1.5 (van Krevelen, 1981), thus z is about 2. By incorporating Eq. (2) into the correction and rearranging, the intensity is multiplied by the factor (1 − a/2)/(1 − a). For the coals here, where the ash yields (expressed as a fraction) are less than 0.2 (hence mineral matter volume fractions less than 0.1), the correction is less than 10%. If the mineral matter porosity contribution to scattering intensity is significant, then analysis of the relationships of the corrected scattering intensity with coal properties should show positive correlations with mineral matter content.

At low R values the scattering intensity has two possible components: incoherent scattering, and heterogeneities in coals on smaller size scales. If the heterogeneity is rank dependent, then I(Q) values at low R should show a rank dependence as well as hydrogen content dependence. Thus I(Q) values were determined at R values of 4, 2.5, 1.7 and 1 nm (the last being the value used to estimate the background). These had the mineral matter correction applied, but not the SLD, since the greater portion of scattering is from hydrogen, whose scattering is not SLD dependent. The I(Q) values were the average of seven points around the nominated Q value. The I(Q) at 4 nm was chosen because it was the point at which the intensities between coals 2 and 5 and the other coals are most marked.

Table 2 lists the α values in the different pore sizes regions and the I(Q) values at different R.

Fig. 7 shows the variation of α in different size regions, plotted against mean maximum vitrinite reflectance (R_v,max). From the errors associated with the individual determinations (Fig. 7) the differences in slope in the different regions is significant, with errors generally greater at the smallest pores sizes. The α(12, 20) values are much more negative, and significantly so, than those in the other regions. In many cases in the high rank coals the slope is close to −4, which is the result for smooth surfaces and suggests that there are few pores in this size range.

Table 3 lists a series of multiple correlation coefficients for the USANS and SANS data. Because the vitrinite and hydrogen content are highly correlated, it is difficult to conclude from these data which of the two parameters is of greater importance in determining neutron scattering properties. Here we will use vitrinite content, whilst recognizing that replacing vitrinite by hydrogen content in the regressions gives relationships equally as significant. A similar problem lies in distinguishing between the two rank parameters carbon content and R_v,max. R_v,max will be used as the rank parameter here.

The only significant relation between the overall slope and the coal properties examined is Rv,max (and carbon content), consistent with the above findings. However, the slopes over narrower size distributions appear to have some contribution by vitrinite. Both R_v,max and vitrinite contributions to α (250, 8000) and α (5, 12) were found to be significant. The relationships found in these two examples were

$$\alpha(5,12) = -2.8 - 0.0066(\pm 0.002)\,\text{vitrinite} - 0.87(\pm 0.16)R_v,\text{max}$$

(plotted in Fig. 8).

$$\alpha(250,8000) = -1.9 - 0.0033(\pm 0.001)\,\text{vitrinite} - 0.17(\pm 0.07)\,R_v,\text{max}.$$

The slopes become increasingly negative as R_v,max (or carbon content) and vitrinite (or hydrogen) content increase. That is, as R_v, max and vitrinite content increase, the fraction of finer pores in these size ranges decreases. The results also show that even though

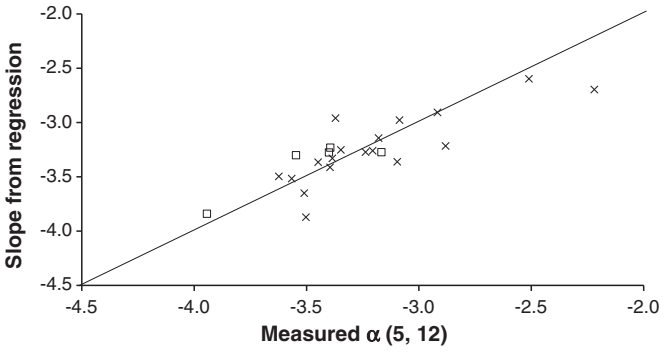

Fig. 8. Relationship between values of α (5, 12) versus those obtained by regression from R_v,max and vitrinite content. (x = Southern hemisphere coals, □ = Northern hemisphere coals).

only R_v,max appears important when the global slope is used, the influence of vitrinite is important in some size ranges.

The influence of R_v,max and vitrinite on scattering intensity I(Q) tends to become stronger with decreasing pore size. This is exemplified in Fig. 9, which shows that there is no obvious relationship between I(Q) at large R with R_v,max, but for smaller pores, the I(Q) value drops by a factor of 5 as the R_v,max increases. Neither R_v,max nor vitrinite play a role in determining the number of larger pores in these coals, but both become increasingly important in finer pores. For example, the relationship between $I(0.01\,Å^{-1})/SLD^2$ (intensity from pores about 25 nm in radius) and both R_v,max and vitrinite content has an r^2 of 0.6.

$$I\left(0.01\,Å^{-1}\right)/SLD^2 = 20.7 - 0.064\,(\pm 0.026)\text{vitrinite} - 8.37\,(\pm 2)R_v,\text{max (plotted in Fig. 9)}.$$

Increasing R_v,max and vitrinite both decrease the intensity of $I(0.01\,Å^{-1})$. Mesopores on the size range 25 nm are increasingly less common as either R_v,max or (to a lesser extent) vitrinite content increases. Vitrinites in general would thus have less mesoporosity than inertinites of the same rank. Fig. 10 shows the relationship between measured values and that predicted from the above relationship. At smaller R values, although some relationships show a high r^2 correlation coefficient, most of the contribution to the variation is by coals 2 and 5. The data analysis also suggests that R_v,max may influence the amount of background scattering observed, as determined by the $I(0.25\,Å^{-1})$ value, but more coals would need to be investigated to confirm this.

Adding mineral matter content as an independent variable produced no significant increase in r^2 coefficient, except in the case of the $I(0.0001\,Å^{-1})/SLD^2$, but again this correlation was strongly influenced by outliers. Coals with a range of mineral matter content would need to be examined to identify any trends. Any influence of mineral matter on coal porosity is overshadowed by the influence of the organic material.

Figs. 8, 9 and 10 also show that the relationships found were not affected by the origin of the coal: The results for Carboniferous Northern hemisphere coals and Permian Southern hemisphere coals overlapped.

3.2. Closed porosity determinations

Measurements of I(Q) were measured at pressure of CD4 required to achieve the zero contrast condition for all of the coals except coal 1.

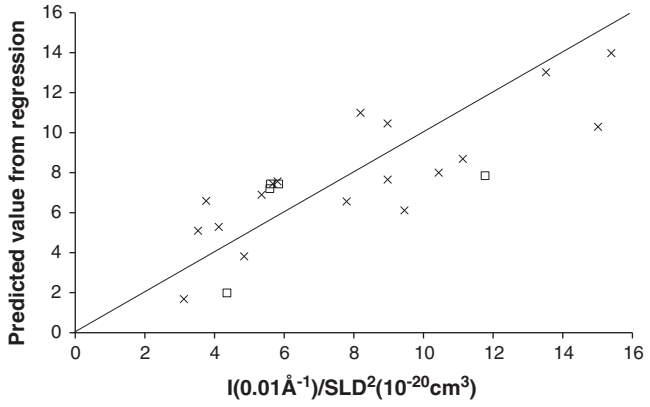

Fig. 9. Value of $I(0.01\,Å^{-1})/SLD^2$ predicted from the regression using Rv,max and vitrinite content versus measured value. (x = Southern hemisphere coals, □ = Northern hemisphere coals.).

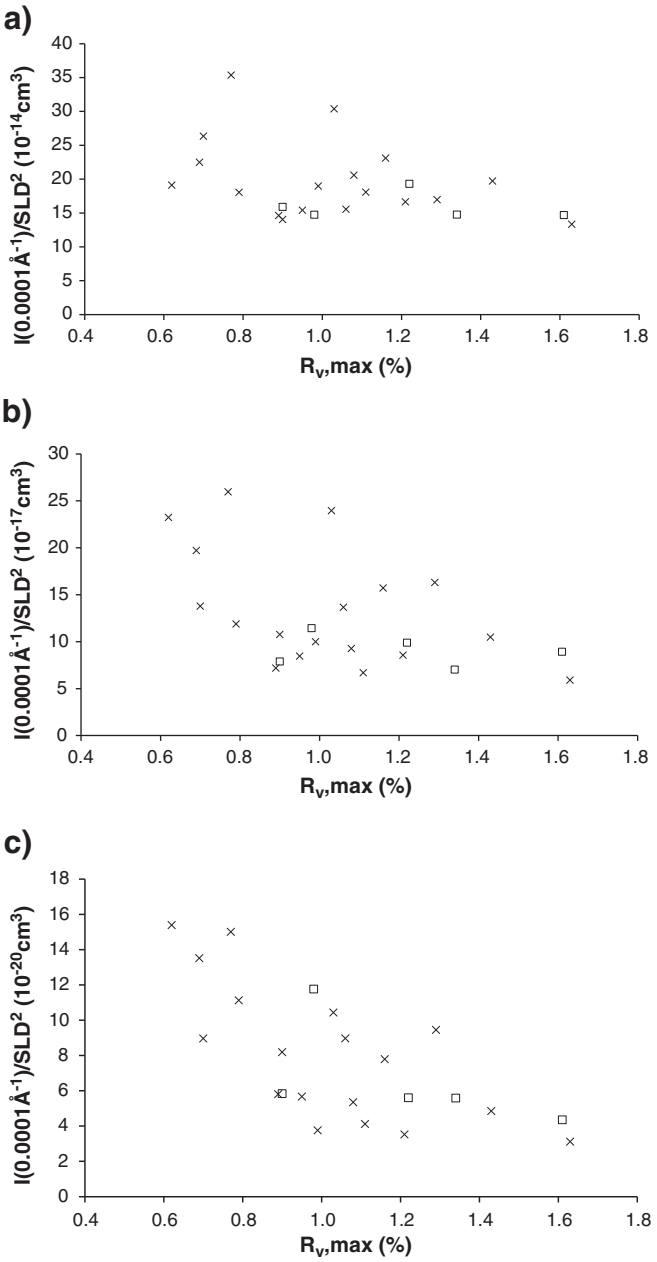

Fig. 10. Relationship between normalized I(Q) values and coal rank at $Q = 0.0001\,Å^{-1}$(a), $0.001\,Å^{-1}$ (b), $0.01\,Å^{-1}$(c). x = Southern hemisphere coals, □ = Northern hemisphere coals. Approximate associated pore radii are 2500, 250 and 25 nm, respectively.

Fig. 11 shows the scattering intensity from coals 8 and 20 in vacuum and in CD_4 at P_{ZC} plotted against R (=2.5/Q). When R > 10 nm, I(Q) decreases when CD_4 is introduced into the coal sample. The remnant scattering from the coal with the CD_4 added at the zero contrast pressure P_{ZC} is caused by inaccessible pores, with possibly some contribution from inhomogenieties in the coal structure.

When R < 10 nm, I(Q) increases slightly in CD_4-flooded coal. This increase has been observed previously using CD_4 in coals (Melnichenko et al., 2012) and is probably caused by condensation of the invading fluid on the pore walls and filling of the micropores. If the condensed phase reaches liquid-like densities (~0.5 g/cm^{-3}), it can introduce scattering length density contrasts with the coal matrix of the same order as that characteristic of empty pore/coal matrix interface. These introduced SLD contrasts can contribute significantly to the flat background if these contrasts occur on a small linear scale

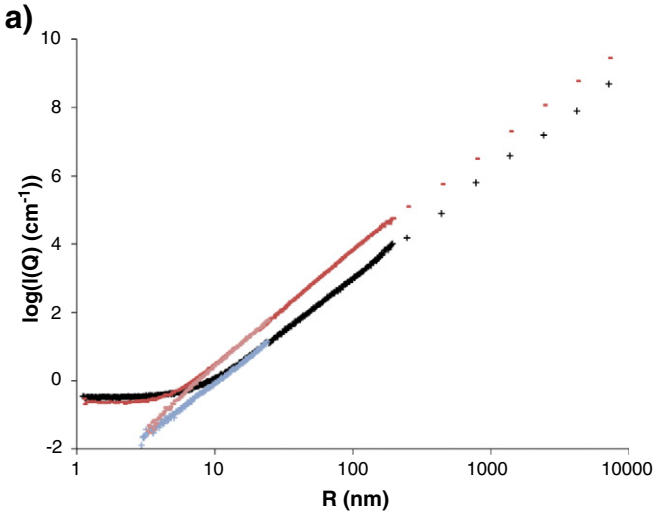

Fig. 11. Neutron scattering intensity (I(Q)) plotted against pore radius R (defined as 2.5/Q) for coal 8 (a) and coal 20 (b) in vacuum (−) and after exposure to CD_4 at the pressure P_{ZC} (+). Intensities corrected for background are shown with paler hues.

(<1 nm). If this flat background is subtracted then the slope is linear down to nearly R~2.5 nm, both in the coals measured in vacuum and exposed to CD_4. However, because at small pore sizes the signal-to-noise ratio of the subtracted curve is poor and I(Q) values become very sensitive to the choice of background intensity, this study of inaccessible pores was restricted to pore radii ≥8 nm.

It is notable that even though the applied pressures of CD_4 are high, there is no evidence of significant density enhancement of CD_4 in pores larger than 2.5 nm (Fig. 11). This suggests that any layer of high-density methane sorbed on surfaces or inside pores is at best only a few molecular diameters thick, even at pressures of the order of 30 MPa. This is consistent with molecular simulations; Vandamme et al. (2010) – in their Fig. 8 – provides a useful pictorial representation of sorption on mesopore surfaces.

Fig. 11 demonstrates also that the response of SANS/USANS intensity to the introduction of CD_4 at the ZC condition is quite different for the two coals (8 and 20). In coal 20, I(Q) at large pore sizes decreases by a factor of five, but the reduction is much smaller as R decreases. In coal 8, the reduction ratio is roughly constant down to at least R of 5 nm. This indicates that the fraction of inaccessible pores as a function of pore size differs greatly between the two coals.

The fraction (fi) of pores that are inaccessible (also called 'closed', or 'blind') to CD_4 is simply the ratio of the intensity of the signal at P_{ZC} to that in a vacuum (or ambient pressure). Fig. 12 shows this ratio for

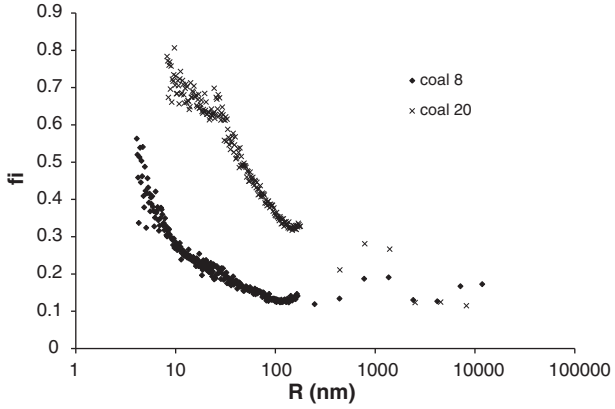

Fig. 12. Fraction of inaccessible pores for the two coals, fi, plotted against R (=2.5/Q) and calculated from the ratio of corresponding, background-corrected, I(Q) values.

the two coals as a function of R. As expected intuitively, the fraction of inaccessible pores increases with decreasing pore size. In both coals, the pores are largely accessible down to 250 nm. However, by 25 nm most (~70%) of the coal pores are inaccessible in coal 20, whereas in coal 8 only 20% are inaccessible. Even at the smallest pore sizes that could be assessed here, in coal 8 most of the coal pores are readily penetrated by methane, but most of the finest pores in coal 20 are inaccessible.

Table 4 lists the fi values (fraction of inaccessible pores) at various pore sizes. These correlate poorly with rank and ash yield at all pore sizes. Fig. 13a and b show the most striking relationship found. At the smallest pore sizes examined, the fi values of the Australian and New Zealand coals increase linearly with hydrogen and vitrinite content; this means that the mesopores are less accessible in the vitrinite-rich coals.

Vitrinite has more hydrogen than inertinite, thus trends of inaccessible pores with both hydrogen and vitrinite are similar. We will confine discussion to vitrinite (Fig. 13b) as the independent parameter here. Since liptinites are largely nonporous (Chalmers and Bustin, 2007), they are combined here with vitrinite to distinguish them from inertinite.

Table 4
Fraction of inaccessible pores at various pore sizes for various coals (background corrected).

R (nm)	8000	2500	800	50	24	12.5	8
2	0.24	0.20	0.16	0.27	0.32	0.29	0.23
3	0.24	0.35	0.36	0.54	0.57	0.53	0.56
4	0.11	0.32	0.65	0.49	0.69	0.69	0.76
5		0.21	0.18	0.14	0.14		
6	0.21	0.20	0.23	0.28	0.40	0.42	0.42
7	0.20	0.09	0.12	0.17	0.25	0.25	0.31
8	0.12	0.13	0.19	0.16	0.23	0.25	0.34
9	0.19	0.21	0.33	0.38	0.58	0.63	0.69
10	0.14	0.10	0.19	0.20	0.27	0.30	0.38
11		0.27	0.35	0.65	0.65		
12	0.12	0.32	0.38	0.86	0.86	0.87	0.92
13	0.20	0.23	0.37	0.52	0.61	0.63	0.68
14	0.14	0.22	0.16	0.40	0.49	0.51	0.64
15	0.19	0.10	0.16	0.41	0.51	0.53	0.63
16				0.30	0.41	0.46	0.60
17	0.25	0.19	0.16	0.42	0.52	0.54	0.61
18	0.19	0.20	0.19	0.50	0.53	0.58	0.68
19	0.39	0.35	0.31	0.38	0.39	0.39	0.45
20	0.11	0.12	0.28	0.45	0.63	0.71	0.83
21				0.78	0.87	0.90	0.87
22	0.16	0.21	0.46	0.70	0.76	0.81	0.87
23	0.14	0.15	0.31	0.64	0.81	0.84	0.84
24	0.15	0.14	0.10	0.56	0.76	0.82	0.90

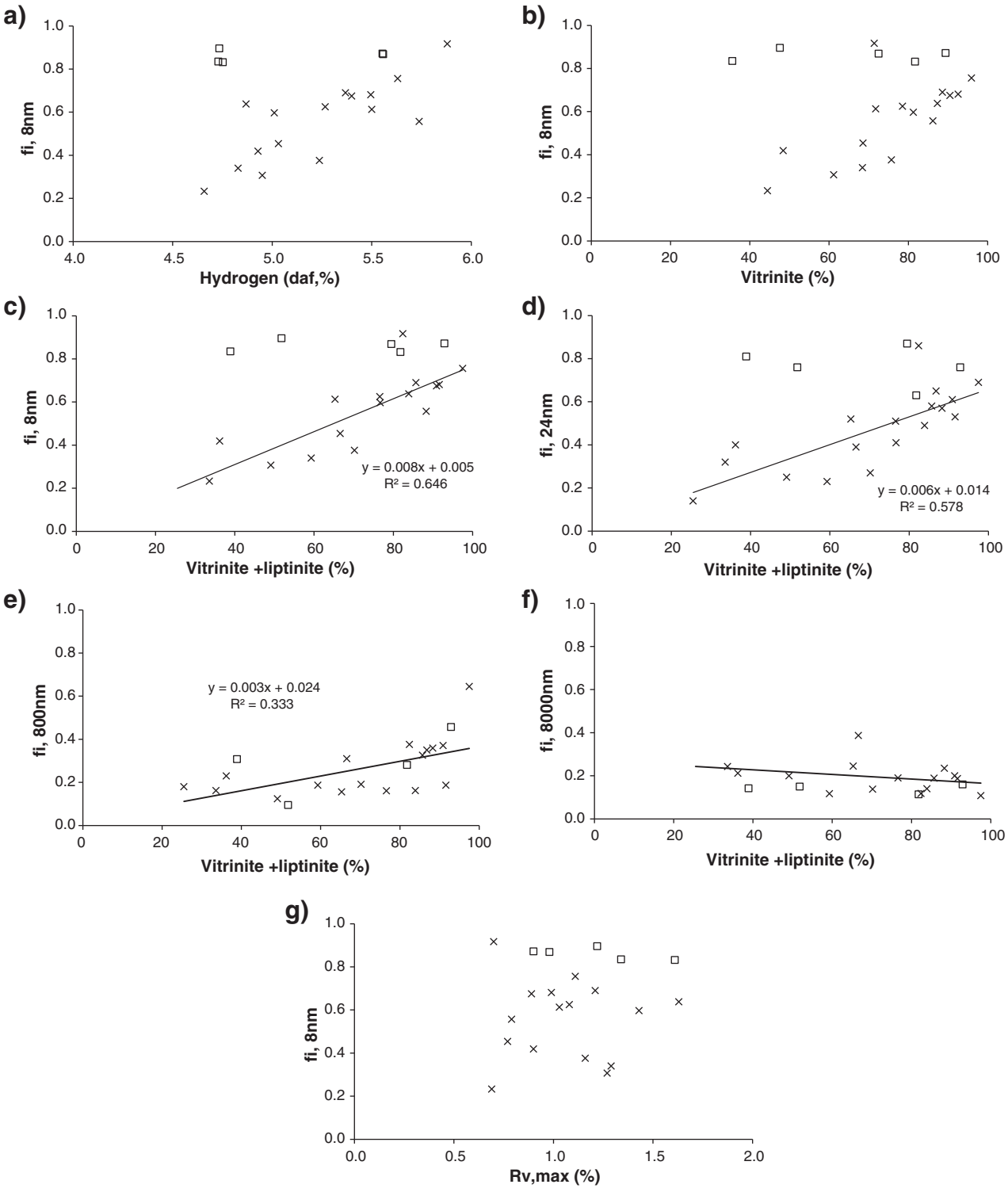

Fig. 13. Relationships between fraction of inaccessible pores (fi) at various pore sizes versus other coal properties. (x = Southern hemisphere coals, □ = Northern hemisphere coals.).

Unlike Australian coals, the 8 nm pores of the Polish and Appalachian coals are found to be largely inaccessible and this inaccessibility was independent of vitrinite content (Fig. 13c and d). However, with increasing pore size, the distinction is lost. At 800 nm (Fig. 13e and f) the fi of the European-American coals cannot be distinguished from the Australian coals by vitrinite content, and the relationship between accessibility and vitrinite has almost completely disappeared; pores of this size are largely accessible whatever the maceral composition. Unlike the results for total pore size distribution, the fraction of coal pores that are inaccessible was not dependent on coal rank (Fig. 13g) over the rank range investigated here.

4. Discussion

4.1. Size distributions of accessible + inaccessible pores

The results here confirm the work of Prinz et al. (2004) that overall α decreases with increasing rank. They also agree with other

findings over a more limited range of coals that high rank coals have less mesoporosity than low rank coals (Gan et al., 1972; Hall et al., 2000). However, the finding that there is a maximum in scattering around 80% carbon near $Q=10^{-3}$ Å^{-1} (Tricker et al., 1983), which was based on 9 coals, is not confirmed (Fig. 14). The change in slope observed for the low rank coals 2 and 6 near $Q=0.01$ Å^{-1} has been observed in a low rank coal previously (Radlinski et al., 2004).

The importance of rank and to a lesser extent maceral composition on the number of pores increases with decreasing pore size. As rank increases, the number of pores around the 25 nm size range decreases by 80% (Fig. 9) and pores in the range 10–25 nm largely disappear. Pores are still evident at smaller size scales in higher rank coals, but the effect of background scattering becomes important and rank influences on total porosity become harder to discern. No conclusions about microporosity (pore size less than 2.5 nm) can be drawn from the SANS data. However, gas sorption studies of coals indicate that microporosity is considerable (Gan et al., 1972). If so, there would appear to be a 'gap' in pore sizes only between 10 and 25 nm in high rank coals.

The abrupt changes in the log–log SANS slope always occur near the same Q values (and, therefore, the same pore sizes), independently of the coal rank or maceral composition. Moreover, slopes in different size ranges do not correlate with each other (Fig. 15), except for α (250, 8000) and α (5, 12), which suggests that differently sized pores are created in a different way. The observed near-fractal behavior of the coal pore structure must therefore originate from a combined effect of different coal formation processes acting on different scales (e.g. the biologically-determined microstructure of the original plant material, fragmentation of the organic debris, diagenesis, grain contact anti-sintering (Cohen, 1987)). The overriding effect of increasing maturation of coal is to reduce the number of fine mesopores, but the data here suggest that a range of mechanisms is operating and this appears to be a rich field for further investigation.

4.2. Size distribution of inaccessible pore fraction

The distinction between the Australian and other coals is clear. The fraction of 8 nm-sized pores in Australian coals that are inaccessible to CD_4 increases linearly with increasing vitrinite content and for the other coals it does not.

The sum of accessible and inaccessible porosity of the coals at 8 nm is weakly related to maceral composition but is strongly related to rank. The fraction of pores at 8 nm that are accessible is related to vitrinite content (at least for Australian coals) but not to coal rank. This indicates that

- The structure in coal that controls access to pores is unrelated to the structure in coal that controls the number of pores themselves.
- Regional influences affect the fraction of pores that are inaccessible but not total porosity.

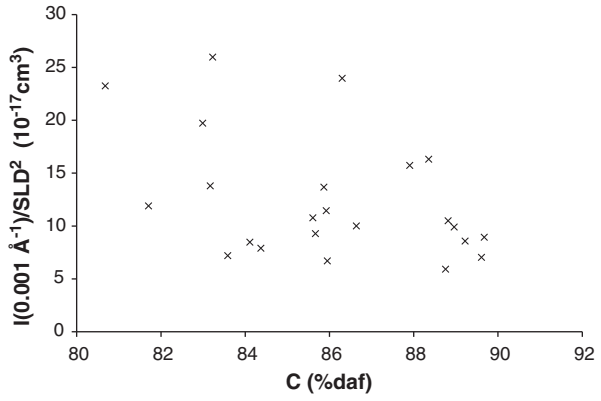

Fig. 14. Relationship between I(0.001 Å^{-1})/SLD^2 and carbon content.

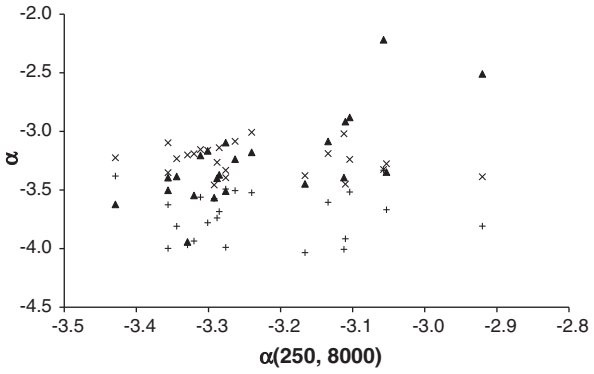

Fig. 15. Relationships between slopes (α) at different pore size ranges with the slope in the size range 250 to 8000 nm (α (250, 8000)). x, α (20,80); +, α (12,20); triangles α (5, 12).

For the Australian coals, plotting the inaccessible fraction against vitrinite + liptinite content (Fig. 13c–e) shows an approximately linear relationship. Extrapolation of the trend line to 0% vitrinite (100% inertinite) gives a value close to zero. This means that when *all* of the Australian coals are considered together, the fine mesopores in inertinite are fully accessible to methane but all vitrinites are about 70% inaccessible. With increasing pore size, more of the pores become accessible; nearly all of the pores of size 800 nm or larger are accessible and the relationship between maceral composition and pore accessibility is weak.

Strikingly, there appears to be a fundamental difference in the nature of the inertinites in Australian and US coals, insofar as gas accessibility is concerned. The Polish and US coals with high vitrinite have similar degrees of accessibility to the Australian coals with high vitrinite. However, it is clear from Fig. 13a–c that the 8 nm pores in the inertinites of the US/European coals are equally as inaccessible as their vitrinites, unlike their Australian counterparts.

One possible cause for this difference is mineralization around pore throats. If so, it would suggest that Carboniferous inertinites have more of this form of mineralization that closes pores than Permian ones. If this were the case, demineralization of coals may be expected to affect the accessibility of American coals to gases more than Australian ones. However, Ozdemir demineralized Argonne premium coals using acid and found only slight increases in sorption capacity (Ozdemir, 2004). In contrast, Massarotto et al. (2010) reported large increases in sorption capacity of two Australian coals – one inertinite-rich and one vitrinite-rich – after exposure to CO_2 at high pressure and excess water, and attributed this to dissolution of minerals. The helium density was relatively unaltered by this treatment, however. They found similar increases in sorption in both coals.

However, if pore throat mineralization controlled inertinite accessibility, it would be unlikely to see a good correlation between pore accessibility and inertinite or hydrogen content. On the contrary, pore accessibility and would be rather determined by the nature of the mineralization encountered by the coal during its maturation and, therefore, should vary strongly between coal samples. We observed no significant correlation with total ash yield, but that may be because the nature of any pore throat minerals may be unrelated to that of bulk ash composition. Thus pore throat mineralization needs to be investigated further as a possibility for reducing pore access.

Another possibility is a structural difference in the inertinite imparted by the different plant origins of the two groups of coals, or the different conditions – temperatures, oxygen levels or salinity – under which they were deposited. If this is the case, then extending this survey to a wider range of coals over a wider range of geological ages would enable relationships between closed porosity and other coal properties to be investigated.

Beamish et al. (1998) suggest that Australian coals can hold more methane than New Zealand coals of the same rank because of the presence of bitumen that binds to surfaces that would otherwise bind methane in the New Zealand coals. Bitumen or surface coatings present in some coals but not others may 'clog' the pore access. If this were the explanation for the difference in behavior of the coals in different regions, this would leave signs visible with SEM or TEM.

The SANS and USANS measurements reported here were performed on a time scale of hours. Equilibration after injection of methane appeared to be rapid (<10 min); no further changes were observed in the SANS results of coals 5 and 11 even after overnight exposure to high pressures of methane. Thus the term 'inaccessible' here is meant to imply 'inaccessible on a time scale of hours'. It is feasible that more of the pores may be accessible to methane on a longer scale. If penetration and release from these pores is possible but slow, permeation into these pores is likely to be thermally activated and could thus be substantially faster at higher temperatures, as is observed for nitrogen sorption near 77 K (Mahajan, 1991) and reported for CO_2 sorption near 0 °C (Radovic et al., 1997).

Much of the gas sorbed by coals is present in a condensed form in micropores (<2 nm) (Gan et al., 1972). These play a major role in gas sorption and release. It is likely that the gas reaches the mesopores in coals through micropores, consistent with the view of coal structure that most pores are accessible only through narrow pores (Radovic et al., 1997). The contribution of micropores to the SANS is not directly observable because their signal is overshadowed by that from incoherent scattering. Their nature is probably distinct from the larger pores, because the linear size of micropores is comparable to the size of coal matrix building blocks (like polyaromatic sheets in higher-rank coals).

Because of this inaccessibility, it seems that extraction of methane from all vitrinite-rich bituminous coals so far investigated would be incomplete. Only coals rich in the forms of inertinite found so far only in Australia would have their methane fully extractable.

This difference in behavior between Carboniferous (US and European) and Permian (Australian) inertinites may help to resolve a difference in the relationships between properties of coals and properties of their cokes that has been found when comparing coals from different regions. These relationships, particularly in the days in which coking coal supply was in excess, were an important commercial debating point in setting the purchase price for the coal (Gransden et al., 1991; Swan et al., 1999).

Coking coals pass through an intermediate plastic phase during their conversion to coke. Many tests that aim to predict coke quality from coal properties use the plastic behavior of coal in their prediction equations. Alternatively, since vitrinites from bituminous coals tend to coke but inertinites do not, relationships based on vitrinite content were also developed. Empirical relationships between coal and coke properties used were found for European and American – Carboniferous – coals. The 'best' cokes required an optimum plasticity (Matsuoka, 1975) or vitrinite content (Nandi and Montgomery, 1975). However, Australian (and Western Canadian) coals produced better cokes than predicted by these relationships (Diessel, 1983; Diez et al., 2002; Gransden et al., 1991; Nandi and Montgomery, 1975; Toryanik et al., 1998). The relationships between coke behavior and vitrinite could be salvaged to some extent when it was recognised that some inertinites did form coke (Diessel, 1983), but the relationships between coke behavior and fluidity could not be reconciled and this led to other approaches to prediction of coke properties being examined.

When a coking coal is heated, it releases volatiles that act as plasticisers. The more readily the volatiles escape, the more the extent of plasticity is reduced (Sakurovs, 2000) – coke will not be formed if fine coal particles are heated in a vacuum. Thus if the volatiles are trapped in the particles, the plasticity of the coal is increased. The inaccessibility of the pores in coals of European and American origin would result in increased plasticity of the particle compared to those in Australian coals, because the rate of escape of volatiles from these closed pores would be retarded. However, in a coke oven, the rate limiting step in plastic coals for escape of volatiles is the rate of escape of these volatiles from the layer in the coke oven that is plastic (Barriocanal et al., 1998; Casal, 2006; Nomura et al., 2010), not the rate of escape from the particle. Coke quality in a coke oven would not be expected to be as sensitive to volatile escape from pores in coals as small scale tests would be. Thus the greater pore accessibility in Australian coal may explain why they would produce better coke than predicted using small scale plasticity tests. If true, then Western Canadian coals could also be distinguishable from Appalachian coals by their mesopore accessibility by methane in their inertinites.

5. Conclusions

A SANS/USANS investigation of 24 bituminous coals has shown that, within the pores of radius 2.5 to 7000 nm, that

- There is a wide range of pore sizes in all of the coals investigated.
- The pore size distribution is strongly affected by rank, with pores in the 2 to 25 nm size range being proportionally less common in higher rank coals. On some pore size scales, decreasing pore number correlated with increasing vitrinite content but this was not true on all size scales.
- The relationships are not influenced by whether the coals are sourced from Australian Permian or Laurasian Carboniferous coals.

Using the ability of USANS/SANS to discriminate between pores that are inaccessible to methane from those that are not, the relationships between inaccessible pores and coal properties were completely different.

We found no correlation between the fraction of closed porosity and vitrinite reflectance at any size scale. This means the mechanism that reduces the number of fine pores during maturation does not affect the access of the remaining pores to methane.

For Australian coals, the accessibility of pores in the size range 8 to 25 nm to methane was related to maceral (or hydrogen) composition. In inertinites, pores of 8 to 25 nm size were fully penetrable by CD_4, whereas the vitrinites were approximately 70% inaccessible. In the studied American and European coals, all pores of this size range were over 80% inaccessible and this did not depend on maceral composition. The mesopores in inertinites of American and Australian coals are very different in their accessibility to methane.

Accessibility of pores to CD_4 in general increased with increasing pore size.

Nomenclature

α	The average slope of the plot of log (I(Q)) versus log Q. When expressed as $\alpha(x_1, x_2)$ it is the average slope between $R = x_1$ and $R = x_2$, where $R = 2.5/Q$. Here α is negative.
a	Ash yield, expressed as a fraction of total mass.
Contrast matching	A technique in which a fluid is added to a porous material at a density selected to give an SLD value the same as that of the material. When the pressure of the fluid is such that the SLD contrast between the fluid and material is zero (the zero contrast condition) there should be no scattering if the fluid has completely penetrated the pore space. Any residual scattering at this density is largely (though not completely) due to pores that are inaccessible to the fluid.
daf	dry ash-free basis. Carbon content, for example, is commonly expressed on a dry, ash-free basis (mass carbon divided by (mass dry coal – mass ash)). Carbon content expressed on a daf basis is more closely related to rank than carbon content expressed on a dry basis.
db	dry basis. Ash yield is usually expressed on a dry basis (mass of ash divided by mass of dried coal).

Ds Surface fractal dimension (=6+α). Provides an indication of the nature of the complexity of the surface roughness.

fi Fraction of pores that is inaccessible to gas. fi varies with Q (or R).

I(Q) The scattering intensity at each Q value. When measured on an absolute scale, the units are inverse length (here cm^{-1}). For a detailed examination of the relationship between I(Q) and pores in materials, see (Radlinski et al., 2000).

mmf mineral matter free basis.

P_{ZC} The pressure of invading fluid at which the zero contrast condition occurs

$Q=(4\pi/\lambda)\sin(\theta/2)$ Scattering vector (units $Å^{-1}$). For SANS, this is the scattering angle normalized for the wavelength of the incident beam). It is related to the pore size (R).

R Pore radius (units nm). For uncorrelated spherical pores that are fractal (i.e. have a broad power law size distribution), the approximate relationship is R=2.5/Q, where pores of sizes centered about R dominate the scattering intensity (Radlinski et al., 2000). R=2.5/Q has been used in this paper. For pores of different shapes and distributions the value of the numerator is model dependent. For example, for stacked slit pores the repeat distance (pore width plus pore wall thickness) is ~2π/Q.

$R_v$max Mean maximum reflectance of vitrinite in the coal when irradiated by polarized green light on a rotatable stage, expressed as a percentage.

θ Scattering angle

SANS Small-angle neutron scattering

SLD Scattering length density. SLD is obtained from the strength of the interaction between neutrons and all nuclei contained in the unit volume of the sample. For some nuclei, notably hydrogen, the SLD value is negative. For homogeneous materials SLD is determined by their chemical composition and mass density.

USANS Ultra small-angle neutron scattering

z Mineral matter density/coal density. Used to convert ash yield (by mass) to ash yield (by volume) in Eq. (2).

ZC The zero contrast condition

Acknowledgements

The research at Oak Ridge National Laboratory's High Flux Isotope Reactor was sponsored by the Laboratory Directed Research and Development Program and the Scientific User Facilities Division, Office of Basic Energy Sciences, U.S. Department of Energy. This research was supported in part by the ORNL Postdoctoral Research Associates Program, administered jointly by the ORNL and the Oak Ridge Institute for Science and Education. The research using the NIST USANS spectrometer was supported in part by the National Science Foundation under agreement no. DMR-0944772. The authors thank Professor Helmut Rauch for his contribution to and support of USANS research on geological materials over the last decade.

References

Barriocanal, C., Patrick, J.W., Walker, A., 1998. The laboratory identification of dangerously coking coals. Fuel 77, 881–884.

Beamish, B.B., Laxminarayana, C., Crosdale, P.J., 1998. Contrasts in Methane Sorption Properties Between New Zealand and Australian Coals. In: Baafi, E.Y., Cram, K., Gibson, G.A., Hanna, P. (Eds.), Proceedings of the 1st Australasian Coal Operators Conference COAL98. University of Wollongong, pp. 561–565.

Casal, M.D., 2006. Influence of the permeability of the coal plastic layer on coking pressure. Fuel (Guildford) 85, 281–288.

Chalmers, G.R.L., Bustin, R.M., 2007. On the effects of petrographic composition on coalbed methane sorption. International Journal of Coal Geology 69, 288–304.

Clarkson, C.R., Bustin, R.M., 1996. Variation in micropore capacity and size distribution with composition in bituminous coal of the Western Canadian Sedimentary Basin: implications for coalbed methane potential. Fuel 75, 1483–1498.

Cohen, M.H., 1987. The Morphology of Porous Sedimentary Rocks. AIP Conference Proceedings, 154, pp. 3–16.

Cui, X., Bustin, R.M., Dipple, G., 2004. Selective transport of CO_2, CH_4, and N_2 in coals: insights from modeling of experimental gas adsorption data. Fuel 83, 293–303.

Day, S., Duffy, G., Sakurovs, R., Weir, S., 2008. Effect of coal properties on CO_2 sorption capacity under supercritical conditions. International Journal of Greenhouse Gas Control 2, 342–352.

Diamond, W.P., Schatzel, S.J., 1998. Measuring the gas content of coal: a review. International Journal of Coal Geology 35, 311–331.

Diessel, C.F.K., 1983. Carbonization reactions of inertinite macerals in Australian coals. Fuel 62, 883–892.

Diez, M.A., Alvarez, R., Barriocanal, C., 2002. Coal for metallurgical coke production: predictions of coke quality and future requirements for cokemaking. International Journal of Coal Geology 50, 389–412.

Gan, H., Walker, P.L., Nandi, S.P., 1972. Nature of porosity in American coals. Fuel 51, 272–277.

Gethner, J.S., 1986. The determination of the void structure of microporous coals by small-angle neutron scattering: void geometry and structure in Illinois No. 6 bituminous coal. Journal of Applied Physics 59, 1068–1085.

Gransden, J.F., Jorgensen, J.G., Manery, N., Price, J.T., Ramey, N.J., 1991. Applications of microscopy to coke making. International Journal of Coal Geology 19, 77–107.

Hall, P.J., Brown, S.D., Calo, J.M., 2000. The pore structure of the Argonne coals as interpreted from contrast matching small angle neutron scattering. Fuel 79, 1327–1332.

Larsen, J.W., 2004. The effects of dissolved CO_2 on coal structure and properties. International Journal of Coal Geology 57, 63–70.

Larsen, J.W., Hall, P., Wernett, P.C., 1995. Pore structure of the argonne premium coals. Energy & Fuels 9, 324–330.

Mahajan, O.P., 1991. CO_2 surface area of coals — the 25-year paradox. Carbon 29, 735–742.

Mares, T.E., Radlinski, A.P., Moore, T.A., Cookson, D., Thiyagarajan, P., Ilavsky, J., Klepp, J., 2009. Assessing the potential for CO_2 adsorption in a subbituminous coal, Huntly Coalfield, New Zealand, using small angle scattering techniques. International Journal of Coal Geology 77, 54–68.

Massarotto, P., Golding, S.D., Bae, J.S., Iyer, R., Rudolph, V., 2010. Changes in reservoir properties from injection of supercritical CO_2 into coal seams — a laboratory study. International Journal of Coal Geology 82, 269–279.

Matsuoka, H., 1975. Requirements for Coals in Japanese Coking Blends. Symposium on Australian Black Coals, its occurrence, mining and preparation. Illawarra Branch of Australian IMM, Wollongong, NSW, Australia, pp. 251–263.

Melnichenko, Y.B., He, L., Sakurovs, R., Kholodenko, A.L., Blach, T., Mastalerz, M., Radliński, A.P., Cheng, G., Mildner, D.F.R., 2012. Accessibility of pores in coal to methane and carbon dioxide. Fuel 91, 200–208.

Mirzaeian, M., Hall, P.J., Jirandehi, H.F., 2010. Study of structural change in Wyodak coal in high-pressure CO_2 by small angle neutron scattering. Journal of Materials Science 45, 5271–5281.

Mohammad, S.A., Arumugam, A., Robinson, R.L., Gasem, K.A.M., 2011. High-pressure adsorption of pure gases on coals and activated carbon: measurements and modeling. Energy & Fuels 26, 536–548.

Nandi, B.N., Montgomery, D.S., 1975. Nature and thermal behaviour of semi-fusinite in Cretaceous coal from western Canada. Fuel 54, 193–196.

Narkiewicz, M.R., Mathews, J.P., 2009. Visual representation of carbon dioxide adsorption in a low-volatile bituminous coal molecular model. Energy & Fuels 23, 5236–5246.

Nomura, S., Mahoney, M., Fukuda, K., Kato, K., Bas, A.L., McGuire, S., 2010. The mechanism of coking pressure generation I: Effect of high volatile matter coking coal, semi-anthracite and coke breeze on coking pressure and plastic coal layer permeability. Fuel 89, 1549–1556.

Ozdemir, E., 2004. Chemistry of the adsorption of carbon dioxide by Argonne premium coals and a model to simulate CO_2 sequestration in coals seams. School of Engineering, University of Pittsburgh, Pittsburgh.

Prinz, D., Pyckhout-Hintzen, W., Littke, R., 2004. Development of the meso- and macroporous structure of coals with rank as analysed with small angle neutron scattering and adsorption experiments. Fuel 83, 547–556.

Radlinksi, A.P., Busbridge, T.L., Gray, E.M., Blach, T.P., Cheng, G., Melnichenko, Y.B., Cookson, D.J., Mastalerz, M., Esterle, J., 2009. Dynamic micromapping of CO_2 sorption in coal. Langmuir 25, 2385–2389.

Radlinski, A.P., 2006. Small-angle neutron scattering and the microstructure of rocks. In: Wenk, H.-R. (Ed.) Russo, J.J. (Series Ed.) Reviews in Mineralogy and Geochemistry. Neutron Scattering in Earth Sciences, 63 (Ch 14), pp. 363–397.

Radlinski, A.P., Boreham, C.J., Lindner, P., Randl, O., Wignall, G.D., Hinde, A., Hope, J.M., 2000. Small angle neutron scattering signature of oil generation in artificially and naturally matured hydrocarbon source rocks. Organic Geochemistry 31, 1–14.

Radlinski, A.P., Mastalerz, M., Hinde, A.L., Hainbuchner, A., Rauch, H., Baron, M., Lin, J.S., Fan, L., Thiyagarajan, P., 2004. Application of SAXS and SANS in evaluation of porosity, pore size distribution and surface area of coal. International Journal of Coal Geology 59, 245–271.

Radovic, L.R., Menon, V.C., Leon, Y., Leon, C.A., Kyotani, T., Danner, R.P., Anderson, S., Hatcher, P.G., 1997. On the porous structure of coals: evidence for an interconnected but constricted micropore system and implications for coalbed methane recovery. Adsorption 3, 221–232.

Sakurovs, R., 2000. Some factors controlling the thermoplastic behaviour of coals. Fuel 79, 379–389.

Sakurovs, R., Day, S., Weir, S., 2010. Relationships between the critical properties of gases and their high pressure sorption behavior on coals. Energy & Fuels 24, 1781–1787.

Setek, M., Wagenfeld, H.K., Stacy, W.O., Kiss, L.T., 1983. Determination of microporosity of brown coal. Small angle X-ray scattering. Fuel 62, 480–482.

Spitzer, Z., 1981. Mercury porosimetry and its application to the analysis of coal pore structure. Powder Technology 29, 177–186.
Swan, A., Thorpe, S., Hogan, L., 1999. Australia–Japan coking coal trade: a hedonic analysis under benchmark and fair treatment pricing. Resources Policy 25, 15–25.
Thimons, E.D., Kissell, F.N., 1973. Diffusion of methane through coal. Fuel 52, 274–280.
Toryanik, E.I., Kaftan, Y.S., Drozsnik, I.D., Kryshen, I.G., Solov'ev, G.D., Futruk, P.Y., Zusmanovskij, A.Y., 1998. On efficiency of utilization of Australian coals for manufacturing the blast furnace coke in Ukraine. Koks i Khimiya 9–15.
Tricker, M.J., Grint, A., Audley, G.J., Church, S.M., Rainey, V.S., Wright, C.J., 1983. Application of small-angle neutron scattering (SANS) to the study of coal porosity. Fuel 62, 1092–1096.
van Krevelen, D.W., 1981. Coal Typology Chemistry Physics Constitution, 2nd ed. Elsevier, Amsterdam.
Vandamme, M., Brochard, L., Lecampion, B., Coussy, O., 2010. Adsorption and strain: the CO_2-induced swelling of coal. Journal of the Mechanics and Physics of Solids 58, 1489–1505.
White, C.M., Smith, D.H., Jones, K.L., Goodman, A.L., Jikich, S.A., LaCount, R.B., DuBose, S.B., Ozdemir, E., Morsi, B.I., Schroeder, K.T., 2005. Sequestration of carbon dioxide in coal with enhanced coalbed methane recovery — a review. Energy & Fuels 19, 659–724.